

Effect of reagent rotation on product energy disposal in the light atom transfer reaction $O(^3P) + HCl(v=2, J=1,6,9) \rightarrow OH(v', N') + Cl(^2P)$

Rong Zhang,^{a)} Wim J. van der Zande,^{b)} Michael J. Bronikowski, and Richard N. Zare
Department of Chemistry, Stanford University, Stanford, California 94305-5080

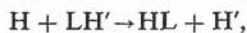
(Received 4 October 1990; accepted 30 October 1990)

A rovibronic-state-to-rovibronic-state experiment has been performed on the reaction $O(^3P) + HCl(v=2, J=1,6,9) \rightarrow OH(v', N') + Cl(^2P)$. The $O(^3P)$ atoms are produced with a known energy by photolysis of NO_2 . The $HCl(v=2, J)$ molecules are prepared by IR excitation of thermal HCl using an optical parametric oscillator. All energetically accessible OH rovibrational product levels are probed by laser-induced fluorescence for each prepared HCl rotational level. The $OH(v'=0, N')$ rotational distribution shows a dip at $N'=11$, the depth of which decreases with increasing HCl rotational excitation. The available energy of reaction is partitioned so that 40% appears as OH vibration (V'), 32% as OH rotation (R'), and 28% as product translation (T'). This energy partitioning does not change with HCl rotation, in contrast to the general expectation for light atom transfer reactions of approximate conservation of internal angular momentum ($R \rightarrow R'$). A substantial vibrational inversion is observed, in agreement with the vibrational adiabaticity ($V \rightarrow V'$) expected for such reactions.

I. INTRODUCTION

Little is known about the effect of reagent rotation upon the partitioning of energy among the degrees of freedom of products of a reaction.¹ In large part, this lack of information has been a consequence of an experimental failing, namely, few studies prepare the reagent in a single rotational level and change this level at will.²⁻⁴ Historically, energy disposal was first studied in detail by Polanyi and co-workers⁵⁻⁹ using infrared chemiluminescence. In addition, Polanyi and co-workers^{6,10,11} carried out classical trajectory studies on model LEPS potential energy surfaces (PES). These studies have been extended by others using both classical¹²⁻¹⁸ and quantum¹⁹⁻²⁶ scattering methods.

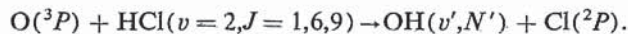
For reactions involving the transfer of a light atom (L) between two heavy-atom partners (H and H'),



a number of trends have emerged concerning energy disposal:

- (1) Translational energy necessary to surmount the reaction barrier is channeled into product vibration ($T \rightarrow V'$),^{10,11}
- (2) Excess translational energy of the reagent is transformed into translational energy and to a lesser extent into rotational energy of the product ($\Delta T \rightarrow \Delta T' + \Delta R'$);^{5,8}
- (3) Excess vibrational energy of the reagent is channeled into excess vibrational energy of the product (vibrational adiabaticity) ($\Delta V \rightarrow \Delta V'$);^{27,28}
- (4) Rotational angular momentum of the reagent is channeled into rotational angular momentum of the product ($R \rightarrow R'$).^{1,19}

In this paper we present a systematic study of the energy disposal in the light atom transfer reaction



The $O(^3P)$ atom is produced with a known kinetic energy by photolysis of NO_2 at 355 nm. The HCl reagent is prepared in a selected $v=2, J$ rovibrational level by IR excitation of thermal HCl . The reaction of $O(^3P)$ with ground state HCl is nearly thermoneutral ($\Delta H_0^0 = 0.9$ kcal/mol or 315 cm^{-1}).²⁹ The height of the barrier for the ground state reaction is not accurately known, but it is believed to be approximately 5.9 kcal/mol. This barrier results in an extremely small room-temperature rate constant of $(1.3 \pm 0.2) \times 10^{-16}$ cm^3 molecule⁻¹ s⁻¹.²⁹ Both experimental³⁰⁻³³ and theoretical³⁴ studies have demonstrated that the room-temperature reaction rate is enhanced strongly by vibrational excitation of the HCl reagent, $k_{HCl(v=1)} : k_{HCl(v=0)} \approx 10^2-10^3$ and $k_{HCl(v=2)} : k_{HCl(v=0)} \approx 10^3-10^4$. The large vibrational enhancement of the $O + HCl$ reactive cross section allows us to study this system using HCl reagents prepared in a single rovibrational state with minimal interference from the thermal reaction.

This paper forms a sequel to an earlier report³⁵ from this laboratory, which contained the first rovibronic-state-to-rovibronic-state study of a chemical reaction. These studies meet one of the goals of reaction dynamics, namely, specifying at will all translational and internal energies of the reagents and measuring these quantities in the nascent products. The results presented in this paper provide a quantitative test of the generalizations previously formulated for energy disposal in light atom transfer reactions.¹ They also provide a stimulus for accurate quantum scattering calculations on reliable potential energy surfaces.

II. EXPERIMENTAL

A schematic diagram of the $O(^3P) + HCl$ reaction apparatus is shown in Fig. 1. Three lasers with a counterpropa-

^{a)} Present address: IBM Almaden Research Center, 650 Harry Road, San Jose, California 95120.

^{b)} Permanent address: FOM-Institute for Atomic and Molecular Physics, Kruislaan 407, 1098 SJ Amsterdam, The Netherlands.

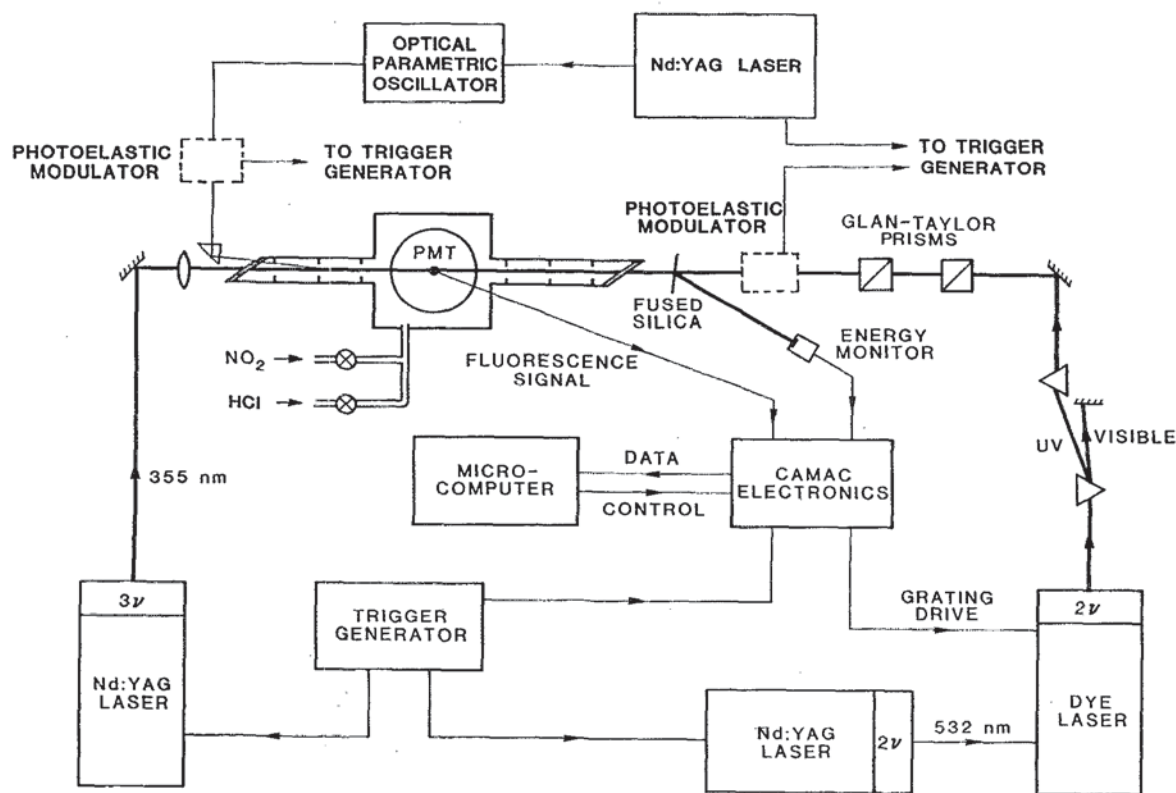


FIG. 1. Schematic diagram of the experimental apparatus for the $\text{O}(^3P) + \text{HCl}(v=2, J) \rightarrow \text{OH}(v', N') + \text{Cl}(^2P)$ reaction.

gating pump-probe geometry are used in our experiments. Briefly, there are two pump lasers and one probe laser. An ultraviolet (UV) laser (40 mJ/pulse, 355 nm, third harmonic from Nd:YAG, Quantel 581) produces the $\text{O}(^3P)$ atoms from photolysis of NO_2 molecules. A tunable infrared (IR) laser prepares the HCl reagent molecules in an excited rovibrational state. The IR light ($\lambda \approx 1.75 \mu\text{m}$) has a bandwidth of approximately 0.1 cm^{-1} at 4 mJ/pulse and is produced in an optical parametric oscillator (OPO) pumped by the $1.064 \mu\text{m}$ fundamental from a Nd:YAG laser (Quanta-Ray, DCR1). The two pump lasers are fired simultaneously and their beams are colinearly directed into the reaction chamber. After a well-defined delay, a third, counterpropagating tunable UV pulsed dye laser beam (Quantel TDL-50 dye laser pumped by a Quanta-Ray DCR2A) probes the OH products using laser-induced fluorescence (LIF).

Individual *R*-branch transitions in the (2,0) band of HCl are identified using both a monochromator (3/4 meter length with a 600 groove/mm grating; SPEX, model 2569) and an optoacoustic cell (fitted with a transducer, PCB Piezotronics Inc., New York, model GK 106B50, together with a preamplifier model 480D06).

Both the photolysis and the probe lasers operate at a repetition rate of 20 Hz while the OPO is synchronously triggered at 10 Hz. This permits alternate shot-to-shot subtraction of background signals, which do not result from rovibrationally excited HCl. The $\text{O} + \text{HCl}$ pump-probe experiment requires extensive signal averaging. At a fixed IR wavelength the dye laser is computer controlled; a very slow

scan rate over the frequency range corresponding to a particular OH *A-X* rovibronic transition peak is combined with fast scanning between adjacent transitions in order to limit the total scan time. The probe laser energy is controlled with Glan-Taylor prisms and monitored on a shot-to-shot basis by a power meter (Moletron J3-05) using a back reflection. We find that the signal-to-noise ratio is also improved by using a slightly saturated probe laser intensity (100 μJ /pulse). For this reason, we have probed OH via the members of the *P* branch, which exhibit rotational line strengths that are constant to within 30% from $N' = 1$ to $N' = 20$.³⁶⁻³⁹ This means that we probe the $\Pi(A')$ Λ -doublet component of the OH $X^2\Pi_{3/2}$ state. For the determination of the $v = 1:v = 0$ vibrational branching ratio, the probe laser is reduced to 15–20 μJ /pulse. This minimized saturation effects.

Fluorescence is collected perpendicular to the common axis of the laser beams by a photomultiplier tube (Centronix 4283/81) through interference filters (chosen to transmit the desired vibronic band of the OH *A-X* transition). The areas under the observed LIF peaks are reduced to relative populations by taking into account the wavelength dependence of the interference filters, the change in probe laser power, and the transition probabilities.^{36,39} Also, a small correction is applied for polarization effects caused by the linearly polarized probe laser.⁴⁰ To check for slow experimental changes, each scan involved a sequence of rotational-line intensity measurements starting and ending on the same rotational line.

A flowing mixture of HCl (Matheson, >99.9% stated purity) and NO₂ (Matheson, >99% state purity) is maintained in the stainless-steel reaction chamber, which is exhausted through a partially throttled diffusion pump. The pressure is monitored by a capacitance manometer (MKS Baratron 222BA, 0–10 Torr). To ensure single-collision conditions, a 1:1 mixture of NO₂:HCl was used at a total pressure of 80–100 mTorr and the pump–probe delay is 150 ns.

III. REACTION ENERGETICS

The O(³P) + HCl reaction is important in the field of combustion science and has been studied by several research groups.^{25–29,31} As mentioned in Sec. I, the reaction of O(³P) with ground state HCl is nearly thermoneutral ($\Delta H_0^0 = 0.9$ kcal/mol or 315 cm⁻¹²⁵). The average total energy available to the reaction products is easily calculated from the following relation:

$$\langle E'_{\text{tot}} \rangle = E_{\text{int}}(\text{HCl}) - \Delta H_0^0 + \langle E_{\text{int}}(\text{O}) \rangle + \langle T \rangle, \quad (1)$$

where $E_{\text{int}}(\text{HCl})$ is the internal energy of the reactant HCl with respect to HCl ($v=0, J=0$), $\langle E_{\text{int}}(\text{O}) \rangle$ is the average internal energy of the reactant O(³P_{*j*}) atom relative to the lowest O(³P₂) level, and $\langle T \rangle$ is the average collision energy of the reactants. Figure 2 presents a diagram of the relative internal energies for reagent and product states. Only the lowest fine structure states [O(³P₂), OH(*X*²Π_{3/2}) and Cl(²P_{3/2})] are shown. The average collision energy is added to the level energies of the reagents. In this way it is easy to read the highest rotational levels accessible in the OH ($v'=0,1$) product.

The O(³P_{*j*}) distribution resulting from the photolysis of NO₂ at 355 nm has been measured using two-photon LIF.^{41,42} We have found a distribution of 0.82:0.15:0.03 for $j=2:j=1:j=0$, respectively. This is colder than the room-

temperature Boltzmann distribution, 0.742:0.208:0.050. The internal energy is 159 cm⁻¹ for the O(³P₁) level, and 226 cm⁻¹ for the O(³P₀) level⁴³). The resulting average internal energy of the O(³P) atoms ($\langle E_{\text{int}}(\text{O}) \rangle$) is negligible (<0.1 kcal/mol).

The average value of the collision energy $\langle T \rangle$ is determined by the photon energy, the NO–O binding energy, and the average NO rovibrational state after the photolysis of NO₂. The NO internal state distribution has been measured by Zacharias *et al.*^{44,45} at a slightly different wavelength from ours (351 nm vs 355 nm). From these data we estimate the average kinetic energy of the photolysis fragments (NO and O) to be about 43% of the maximum available energy of 3690 cm⁻¹.⁴⁵ In order to obtain the collision energy T in the O–HCl center of mass the transformation must be made to the O + HCl center-of-mass system. We estimate an average collision energy of 1100 cm⁻¹. In calculating this average collision energy for reaction, we have included a barrier of 2.2 kcal/mol. This is based on the trajectory studies of Persky and Broida,¹² who found that the reactive cross section is essentially zero at lower collision energies. Thus, the average collision energy of reactive scattering is higher than the average collision energy for all scattering events. The spread in collision energy is determined by the distribution over NO rovibrational states and by the effect of the thermal motions of NO₂ and HCl on the collisions between the hot O atoms and HCl. The importance of this source of collision energy spread for hot atom reactions has recently been discussed.⁴⁶ The two combined effects result in an estimated FWHM spread of 3.2 kcal/mol (or 1120 cm⁻¹).

Despite this sizable spread in the collision energy, the total available energy for the reaction products is well defined (FWHM 14% uncertainty). This energy is dominated by the rovibrational energy in the selectively excited HCl ($v=2, J$) level. Table I compiles the energetics for the different HCl ($v=2, J$) rotational levels studied. Note the relatively small increase of total available energy by increasing the HCl rotational quantum number from $J=1$ to $J=9$. This increase of energy is comparable to the FWHM spread in the collision energy. The concentration of selectively excited HCl molecules depends on the product of the rota-

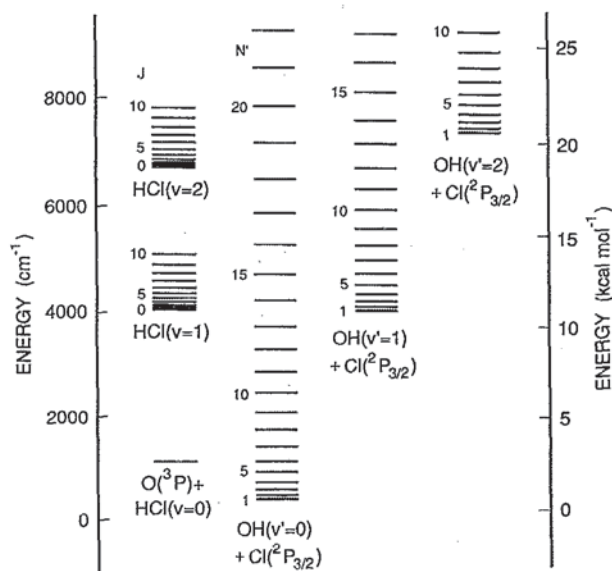


FIG. 2. Energy diagram for the O(³P) + HCl → OH(*X*²Π; v', N') + Cl reaction system. The zero reference energy is measured with respect to the reagents in their lowest internal states. At the reagent side the average collision energy is added (see the text).

TABLE I. Reaction energetics for O + HCl ($v=2, J$) and O + HBr (thermal) in kcal/mol.

	O + HCl			O + HBr
ΔH_0^0	0.9			-14.7
$E_{v=2}$	16.2			...
$\langle E_{\text{coll}} \rangle$	3.2			4.0
$E_{\text{coll}}^{\text{max}}$	4.8 ^a			5.6
$\langle E_{\text{int}}(\text{O}) \rangle$	0.09			0.09
<i>J</i>	1	6	9	Thermal
E_r	0.06	1.3	2.7	1.4
$\langle E'_{\text{tot}} \rangle$	18.6	19.8	21.2	20.1
$E'_{\text{tot}}^{\text{max}}$	20.2	21.4	22.8	21.9

^a $E_{\text{coll}}^{\text{max}}$ is determined by adding the HWHM of the collision energy distribution to its average value.

cited HCl molecules depends on the product of the rotational population of the HCl molecules in the ground vibrational state and the line strength. We have studied OH product distribution for HCl ($v = 2, J = 1, 6, 9$). The thermal rotational distribution of HCl peaks at $J = 3$ and the population at $J = 8$ is only 10% of that of the $J = 3$ level. Therefore, we were limited to preparing HCl ($v = 2, J$) for $J < 10$. The rotational levels $J = 1, 6, 9$ have been chosen because these levels are approximately equidistant (500 cm^{-1}). It is interesting to note that in the study of the $\text{O} + \text{HBr}$ system by our laboratory^{47,48} nearly the same total energy was available. The corresponding energetics of this reaction are also given in Table I.

IV. RESULTS

A. Data acquisition

Careful checks have been carried out to ensure that single-collision conditions hold. The pressure P and delay Δt between the firing of pump lasers (for photolysis and ir excitation) and the probe laser is chosen to prevent significant collision relaxation of the reagent and the product. At $P\Delta t$ values of $< 2 \times 10^{-8}$ Torr s unrelaxed OH distributions with a reasonable signal-to-noise ratio were observed. It was found that within the range of 1×10^{-8} to 4×10^{-8} Torr s for $P\Delta t$ the relative line intensities of $P_2(6)$, $P_1(7)$, and $Q_1(12)$ transitions of the OH $A-X(1,1)$ band remained identical. It is also important to minimize the total pressure to avoid quenching of the OH A state during its relatively long fluorescence lifetime (about 750 ns ^{36,39}). Within our signal-to-noise ratio, it is found that the measured distributions are insensitive to the total pressure in the range of 50–100 mTorr for a 1:1 mixture of HCl:NO₂. Therefore, a delay time of 150–200 ns and a total pressure of 80–100 mTorr were used.

Representative OH spectra produced by the reaction of $\text{O}(^3P) + \text{HCl}(v = 2, J)$ are presented for $J = 1$ in Fig. 3(a) and for $J = 9$ in Fig. 3(b). These spectra cover the P_1 branch of the OH $A-X(0,0)$ band from $N' = 13$ –19 and two lines from OH $A-X(1,1)$ bands ($P_1, N' = 8; P_2, N' = 7$). The spectra of Fig. 3 show that the OH ($v' = 0$) product has a substantial amount of rotational energy for both HCl ($v = 2, J = 1$) and HCl ($v = 2, J = 9$). Moreover, the population in OH ($v' = 1$) increases with increasing reagent HCl rotational excitation.

The effect of rotation on the reaction cross section contains valuable information on the reaction dynamics. For example, Kornweitz *et al.*⁴⁹ have related steric hindrance with the dependence of reactivity on rotation in $\text{O} + \text{HCl}$. Using the measured line intensities and the known rotational line strengths for these transitions, we estimate that the total reaction cross section increases by a factor of 1.5 ± 0.5 as HCl ($v = 2, J$) goes from $J = 1$ to $J = 9$. The large uncertainty represents the difficulty of ensuring the overlap of all three laser beams and the lack of knowledge about the change in the OPO bandwidths. This should be an improvement upon the previous preliminary estimate³⁵ for this enhancement factor, which did not take into account all OH states populated.

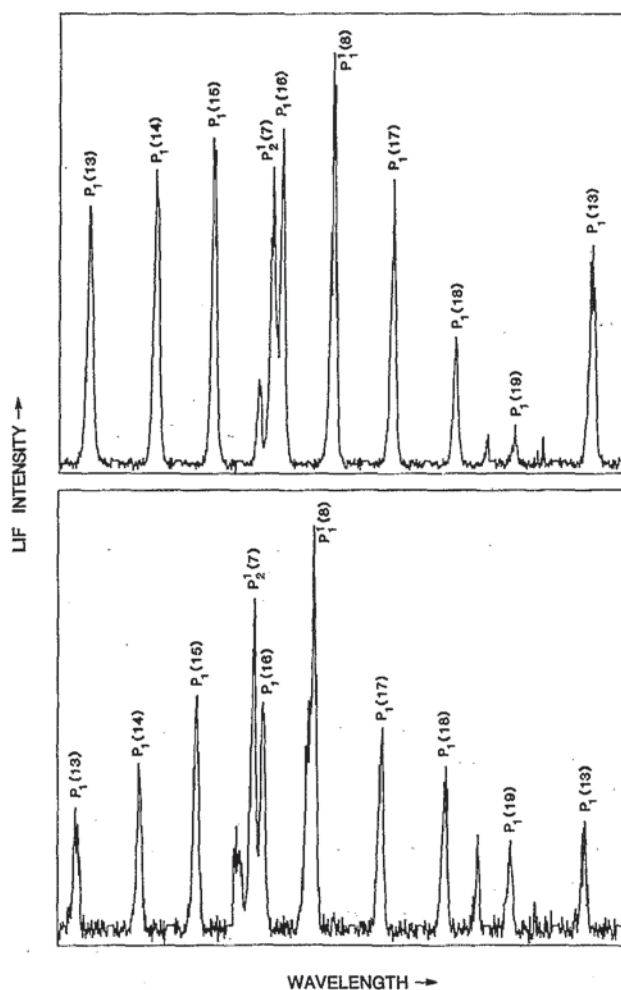


FIG. 3. LIF excitation spectrum of the OH $A-X(0,0)$ and OH $A-X(1,1)$ transitions from the reaction $\text{O}(^3P) + \text{HCl}(v = 2, J)$ for (a) $J = 1$ and (b) $J = 9$. The spectrum consists of multiple short scans of 0.05 nm over individual rotational transitions with frequency jumps between them. In the spectrum, P_1 denotes the OH $A-X(0,0)$ transition and P_1^1 denotes the OH $A-X(1,1)$ transition, etc.

B. Internal energy distributions of the OH product

The (v', N') populations of the OH $^2 \Pi_{3/2}$ product are obtained from a large number of measured and integrated spectra. The results are presented in Figs. 4 and 5 for $v' = 0$ and $v' = 1$, respectively. The population for each N' is plotted against its total rovibrational energy. In each figure the results for selectively exciting HCl in $v = 2, J = 1, 6, 9$ are compiled. The distributions are normalized by equating to unity the sum of populations over the $v' = 0$ and $v' = 1$ rotational levels:

$$\sum_{v'=0,1; N'=N'_{\min}}^{N'=N'_{\max}} P_J(v', N') = 1. \quad (2)$$

$P_J(v', N')$ is the relative population of OH products in a specific rovibrational state (v', N') resulting from reaction with a prepared rotational state J of HCl ($v = 2$). The errors on relative rotational populations are estimated to be ap-

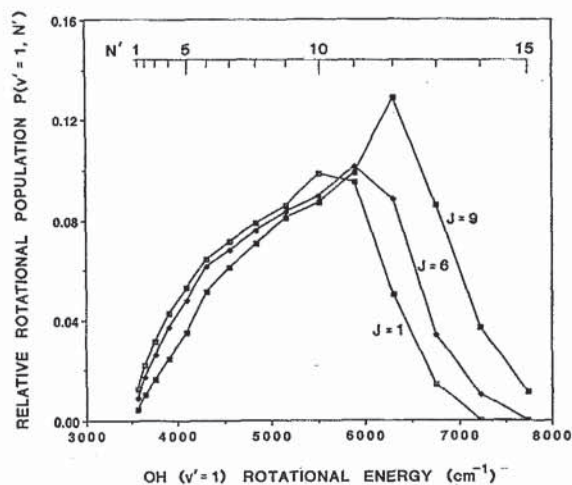


FIG. 4. Relative rotational state populations $P(v', N')$ of the product OH formed in the $X^2\Pi_{3/2} (v'=0)$ ground state from the $O(^3P) + HCl(v=2, J)$ reaction with $J=1, 6, 9$. The normalization of the curves is discussed in the text.

proximately 10% for each measured state. In addition to a background reaction (see below), other sources of experimental uncertainty are the power fluctuations of the OPO and to a lesser extent the photolysis and dye lasers, instability of the flow rates of the two reagents, and the ratio of the reagent mixture.

The dynamical information of this experiment is contained in Figs. 4 and 5. The OH ($v'=0$) and OH ($v'=1$) rotational distributions both peak at high rotational levels. The maxima of both distributions are close to the highest (v', J') level that can be energetically populated using the total energy available in each case, thus leaving little energy for product recoil (see Fig. 2). For example, for HCl ($v=2, J=9$) the maxima in the rotational population distributions occur at $N'=20$ for OH ($v'=0$) and at $N'=15$ for OH ($v'=1$). These levels have an energy of approxi-

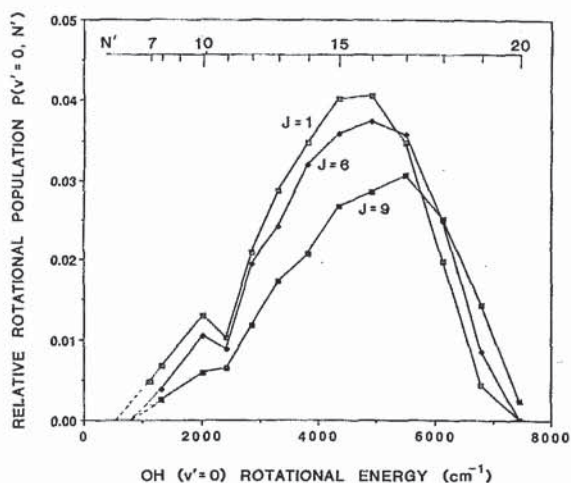


FIG. 5. Relative rotational state populations $P(v', N')$ of the product OH formed in the $X^2\Pi_{3/2} (v'=1)$ state from the $O(^3P) + HCl(v=2, J)$ reaction with $J=1, 6, 9$. The normalization of the curves is discussed in the text.

mately 22 kcal/mol (7700 cm^{-1}), which is slightly higher than the estimated average total available energy.

For OH ($v'=0$) and OH ($v'=1$), the maxima in the rotational distributions shift to higher values as the reagent HCl rotational energy increases. However, the rotational quantum number of each maximum only shifts by one or two units of angular momentum, while the reagent rotational quantum number is increased by eight. The observed increase reflects the increased amount of available energy.

The falloff of the rotational populations at high N' values is remarkably similar to the falloff in the spread of collision energies (1.6 kcal/mol , 560 cm^{-1} HWHM), suggesting that the nascent distribution at a better defined collision energy might peak at the highest accessible product rotational level.

In Fig. 4, the rotational distributions are extrapolated for OH ($v'=0, N' < 7$). Background OH signal, which results from contamination of the NO_2 gas (presumably water, yielding gas-phase HNO_3), prevented us from taking reliable data at smaller N' values. The 355 nm laser pulse efficiently photolyzes HNO_3 molecules to produce OH and NO_2 . The OH molecules are formed in $v'=0$ peaking at $N'=0$.⁵⁰ The highest rotational state populated in these OH radicals is $N'=13$. Our method of shot-to-shot subtraction (OPO on vs OPO off) allowed us to take data for OH ($v'=0, N' > 7$) for reaction with HCl ($v=2, J=1$), and for OH ($v'=0, N' > 8$) for reactions with HCl ($v=2, J=4, 5, 6, 9$). It should also be noted that P_1 transitions for the OH ($v'=0, N'=9$) and OH ($v'=1, N'=8$) levels could not be obtained because of overlap with other transitions.

The reaction exoergicity of the $O + \text{HBr}$ reaction nearly equals the rovibrational energy of the prepared HCl level in the thermoneutral $O + \text{HCl}$ reaction.^{47,48} In the $O + \text{HBr}$ case, no OH ($v'=0$) was found, whereas 90% of the product is in OH ($v'=1$) and 10% in OH ($v'=2$). This observation compelled us to look for signal in the $v'=2$ state. However, no OH ($v'=2$) was observed for $O(^3P) + HCl(v=2, J)$.

C. Nonmonotonic rotational distribution in OH ($v'=0$)

Figure 4 shows the rotational distribution for the OH ($v'=0$) product. A dip occurs at $N'=11$, which is most pronounced when HCl is prepared in $v=2, J=1$ and has nearly disappeared when HCl is selected in $v=2, J=9$. We have also observed this dip for HCl prepared in $v=2, J=4$. We have repeated experiments near the dip and reduced the experimental uncertainty to approximately 6%. This dip cannot be attributed to the optical system for observing the OH product because the same setup was used to carry out experiments on the $\text{H} + \text{O}_2$ reaction,⁵¹ where a smooth monotonic distribution was found. We have not been able to attribute the observed nonmonotonicity to any other effect than unusual dynamics in the $O + \text{HCl}$ reaction. At this point we have no satisfactory explanation why this dip occurs.

Koizumi and Schatz have recently carried out one-dimensional and three-dimensional quantum-mechanical

scattering calculations for $O(^3P) + HCl(v=1)$ on a LEPS surface^{23,24} and more recently on a parametrized *ab initio* surface.⁵² In these studies they have characterized resonances in the reaction probability as a function of the total available energy. These resonances reflect a spectrum of metastable internal states of the O–H–Cl reaction complex. The energy definition in the present study (a FWHM estimate of 3.2 kcal/mol) makes it seem unlikely that resonances, which typically have a width of a few cm^{-1} , would survive in our experiments. More calculations remain to be carried out for the $O(^3P) + HCl(v=2, J)$ reaction to allow a comparison with our results.

V. DISCUSSION

A. Energy disposal

From the results shown in Figs. 4 and 5, the disposal of the available reaction energy into vibration and rotation is easily deduced. The remainder is attributed to translation of the products. The product vibrational, rotational, and translational energies are given in Table II; as can be readily seen, the energy of each degree of freedom increases with increasing rotation of $HCl(v=2)$. Table II also lists the *relative* contribution of the different degrees of freedom to the total energy of reaction. These relative contributions, $\langle f'_i \rangle$, are defined as

$$\begin{aligned}\langle f'_V \rangle &= \langle V' \rangle / \langle E'_{\text{tot}} \rangle, \\ \langle f'_R \rangle &= \langle R' \rangle / \langle E'_{\text{tot}} \rangle, \\ \langle f'_T \rangle &= \langle T' \rangle / \langle E'_{\text{tot}} \rangle.\end{aligned}\quad (3)$$

TABLE II. Energy partitioning and average fractional energies of the products for the $O(^3P) + HCl(v=2, J)$ reaction. For comparison the results for $O + HBr(v=0, J)$ thermal) are listed.^a All energies are in kcal/mol.

<i>J</i>	O + HCl			O + HBr
	1	6	9	Thermal
<i>V</i>	16.2	16.2	16.2	0
$\langle T \rangle$	3.2	3.2	3.2	4.0
<i>R</i>	0.06	1.3	2.7	1.4
ΔH_0°	-0.9	-0.9	-0.9	14.7
$\langle E'_{\text{tot}} \rangle$	18.6	19.8	21.2	20.2
$\langle V' \rangle^b$	7.3	7.6	8.2	11.7
$\langle R' \rangle^c$	5.9	6.4	7.0	5.5
$\langle T' \rangle^d$	5.4	5.8	6.0	3.0
$\langle f'_V \rangle$	0.87	0.82	0.76	0
$\langle f'_R \rangle$	0.17	0.16	0.15	0.19
$\langle f'_T \rangle$	0.003	0.06	0.13	0.07
$\langle f'_{\Delta H_0^\circ} \rangle$	-0.05	-0.05	-0.05	0.73
$\langle f'_V \rangle$	0.395	0.386	0.386	0.58
$\langle f'_R \rangle$	0.320	0.325	0.331	0.27
$\langle f'_T \rangle$	0.285	0.289	0.284	0.15

^a References 47 and 48. The numbers are slightly different because of a re-evaluation of $\langle T \rangle$.

^b $\sigma_{V'} = 0.2$ kcal/mol.

^c $\sigma_{R'} < 0.2$ kcal/mol.

^d $\sigma_{T'} = 1.6$ kcal/mol.

The experimental errors are only 1%–2%, although larger systematic errors are possible from uncertainties in the vibrational band strengths.³⁶ The energy available for reaction is dominated by reagent vibration. The product energy disposal, however, is not only remarkably insensitive to the extra rotational excitation of the HCl reagent, but even shows approximate equipartition of the available energy over all degrees of freedom. This is in sharp contrast not only to the initial conditions prior to reaction but also to the conservation of rotational angular momentum, formulated as being characteristic for light atom transfer reactions.^{1,19} Figure 6 illustrates the energy partitioning for the $O(^3P) + HCl(v=2, J)$ reaction as a function of the initial rotational energy of the HCl reagent.

Two remarks must be made at this point. Only levels of OH ($X^2\Pi_{3/2}$) having *A'* symmetry have been probed. It has been found that the energy disposal over the recoil and internal energies of the products in simple reactions is very similar for the different OH spin-orbit components, but may vary for the Λ -doublet components.^{51,53,54} Second, we have not taken into account the chlorine atom fine-structure splitting of 881 cm^{-1} .⁴³ In our experiment the product ratio between the Cl (2P_j) fine-structure levels has not been probed. The entries in Table II refer to Cl ($^2P_{3/2}$) product atoms. If the chlorine product is preferentially formed in the excited spin-orbit state, the fraction of product translational energy (*T'*) would be reduced by approximately 25%, and the fraction of energy in product recoil would change from 0.29 and 0.21.

Vibrational inversion of product molecules is probably the most characteristic feature in the product distribution for light atom transfer reactions. The observed vibrational branching ratios, OH ($v'=1$)/OH ($v'=0$), are 2.6 ± 0.1 , 3.0 ± 0.1 , and 4.1 ± 0.2 with the HCl ($v=2$) reagents prepared in $J=1, 6$, and 9 , respectively. These numbers have a much firmer basis than those presented in an earlier report.³⁵ It is clear that vibrational inversion increases dramatically with the available energy. However, the steep increase in the

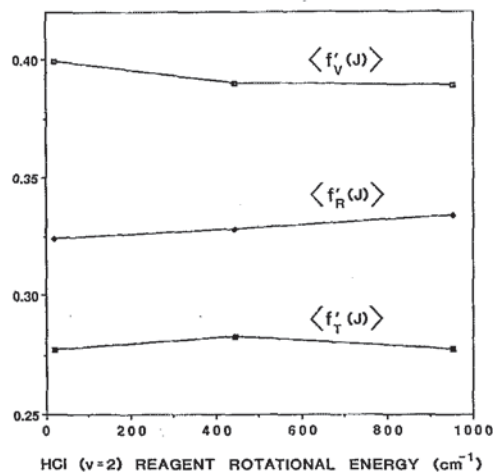


FIG. 6. The fractional energy disposal into products from the reaction $O(^3P) + HCl(v=2, J)$ as a function of reagent rotational energy.

vibrational inversion only reflects a constant fraction of energy in product vibration (see Table II).

Comparison with the analogous reaction, $\text{O} + \text{HBr}$ (thermal) $\rightarrow \text{OH} + \text{Br}$, shows both similarities and differences in the energy disposal. In both reactions the OH product shows strong vibrational and rotational excitation. However, closer inspection shows that the OH product from $\text{O} + \text{HBr}$ is much more vibrationally excited than from $\text{O} + \text{HCl}$ ($v = 2$). Indeed, no OH ($v' = 0$) is observed in the former reaction whereas 25%–40% of the OH product is in OH ($v' = 0$) for the latter reaction. These differences suggest that kinematics⁵⁵ alone does not describe these light atom transfer reactions, i.e., there are significant differences in the corresponding potential energy surfaces. As will be discussed later, this may represent a difference in the geometry of the transition state.

B. Vibrational adiabaticity

Vibrational adiabaticity has been observed in calculations of light atom transfer reactions^{15,16,20,21,23} in which the vibrationally excited reagents cut the corner of the PES, enabling efficient conversion of reagent vibration into product vibration. It is especially prevalent in symmetric reactions where the vibrational constant is the same in the reagents and products. For the $\text{O} + \text{HCl}$ system the vibrational constants differ: 3735 cm^{-1} for OH and 2985 cm^{-1} for HCl. Therefore, pumping two quanta of vibration in the HCl reagent is not necessarily sufficient to form OH product molecules in $v' = 2$. The fraction of energy appearing in vibration can be strongly influenced by the quantized nature of the vibrational motion. For example, upon preparing HCl ($v = 2, J = 1$), the total available energy is insufficient to produce OH ($v' = 2$) products. Even if OH ($v' = 1$) is formed, only 58% of the available energy appears in product vibration.

The occurrence of vibrational inversion indicates that a direct abstraction mechanism is involved without the formation of a long-lived complex. Qualitatively, the present result supports the trends [(1) and (3) of Sec. I] commonly attributed to light atom transfer reactions. The third trend ($\Delta V \rightarrow \Delta V'$) seems applicable, since most of the available energy of reaction is in reagent vibration.

C. Reagent rotation

A key result of our study is that reagent rotation is distributed almost equally over all degrees of freedom of the products, i.e., is not channeled into product internal rotation. This is in sharp contrast with the fourth trend given in Sec. I. The validity of this last trend had been questioned by Schatz *et al.*²⁰ who provided a counterexample in their quantum study of $\text{Cl} + \text{HCl}$. Moreover, for the $\text{O} + \text{HCl}$ ($v = 1$) reaction Koizumi and Schatz^{23,24} found that the OH (v', N') rotational distribution is qualitatively unchanged as a function of the HCl rotation. A rationalization of these observations can be provided using the following relation between reagent and product angular momentum:⁵⁶

$$\mathbf{J}' = \sin^2 \chi \mathbf{L} + \cos^2 \chi \mathbf{J} + \cos^2 \chi \mathbf{d}, \quad (4)$$

where \mathbf{L} and \mathbf{J} are the $\text{O} + \text{HCl}$ orbital and HCl internal angular momenta, \mathbf{J}' is the OH internal angular momentum, and χ is the skew angle.⁵⁵ In Eq. (4), \mathbf{d} describes the dynamics; this vector depends on the changes in internuclear separation during the collision. The last term is important in the case of light atom transfer because of both the high velocity of the light atom and the $\cos^2 \chi$ factor. For example, even during a “direct” abstraction reaction, trajectory studies^{11,12,14,17} show that secondary encounters of the “fast” hydrogen atom with both heavy atoms frequently occur. These secondary encounters may also explain why the energy disposal in the $\text{O} + \text{HCl}$ reaction has essentially no memory of the reagent rotation, resulting in a near equipartition of the excess rotational energy into product vibration, rotation, and recoil.

The present results show that the internal rotation of the OH product does not originate from the reagent rotation \mathbf{J} but from dynamical effects, such as torques on the diatomic product during the reactive collision as described by the vector \mathbf{d} . Intuitively, it is likely that product rotation is sensitive to details of the PES. If repulsive forces work on the light atom during the breakup of an even slightly bent H–L–H' complex, rotation of the LH' product is efficiently induced by the long lever arm. High product rotation is a common feature in hydrogen atom transfer reactions. However, in studies by Kleinermanns and Luntz⁵⁷ of $\text{O}(^3P)$ reactions involving hydrogen abstraction from heavy organic compounds, very little OH product rotation is found. This phenomenon is explained by steric effects that prevent a departure from colinearity of the reaction complex. The present study illustrates that product rotational distributions do contain information on the PES and also are not dominated by kinematic constraints for a light atom transfer reaction.

D. Comparison with theory

Elofson and Holmlid¹⁸ have recently used a statistical algorithm method to describe the $\text{O}(^3P) + \text{HCl}$ ($v = 2, J$) reaction.³⁵ Their model assumes that this reaction proceeds via a long-lived intermediate complex. This contradicts our conclusion that a direct reaction mechanism is involved. Although their OH ($v' = 1$) rotational distributions are in good agreement with our experiment, their OH ($v' = 0$) rotational distributions are too hot. More importantly, their simulation predicts an OH ($v' = 1$)/OH($v' = 0$) ratio of 0.67, in strong disagreement with the OH vibrational inversion found in this study.

Persky and co-workers^{12–17} performed a series of quasi-classical trajectory studies on light atom reactions of the type $\text{O}(^3P) + \text{HX}$ ($X = \text{I}, \text{Br}, \text{Cl}$) employing different types of LEPS potential energy surfaces. In all cases a linear minimum energy path is assumed. Two LEPS PESs were found that reproduced the increase of the rate constants in the $\text{O}(^3P) + \text{HCl}(v)$ reaction with v . The product rotational distributions, however, are completely different for these two LEPS PESs. In a previous report from this laboratory³⁵ it has been concluded that their LEPS surface I^{12,13,17} is in much better agreement with the observed rotational product distribution than LEPS surface II, which predicts hardly

any energy disposal in product rotation. Quantitatively, Persky and Broida¹² predict for the $O(^3P) + HCl(v=2, J$ thermal) reaction that the available energy is distributed 58% in product vibration, 14% in product rotation, and 28% in product translation. Their results clearly underestimate the amount of product rotation. Kornweitz and Persky¹⁴ have addressed the effect of reagent rotation on product rotation on their LEPS-I PES. For $O + HCl(v=2, J=0)$, 15% of the available energy is channeled in product rotation and for $HCl(v=2, J=10)$ this fraction increases to 17%. In contrast, we do not observe any significant effect of reagent rotation on the fraction of available energy disposed in product rotation.

Schecter and Levine⁵⁸ have suggested that the enhancement of reaction rate with HCl vibration is caused in part by an enlarged reactive cone of acceptance. Thus, more trajectories will sample bent trajectories, which results in product rotation. This effect is present in the trajectory studies of Persky and co-workers. Apparently, classical trajectory studies on LEPS surfaces are not able to reproduce our experimental results. This may be caused by the quantum nature of the reaction or by an incorrect representation of the true PES by a LEPS surface having a linear minimum energy path.

Recently, Gordon *et al.*⁵⁹ have performed *ab initio* calculations for the $O + HCl$ reaction. The PES has a bent transition state and hence gives enhanced product rotation. The electronic state has $^3A''$ symmetry. While there is some variation in the predicted $H-Cl$ bond length at the saddle point, there is good agreement among the calculational methods used that the $O-H-Cl$ angle is about 138° . The large rotational excitation is present even at the cost of product vibration. This may provide a partial explanation for differences between $O + HBr$ and $O + HCl$ in that one transition state may be more bent than the other. We await new detailed reactive scattering calculations on an improved potential energy surface to compare with the present results.

VI. CONCLUSION

There exists a widespread interest in understanding the effect of available reagent energy on product energy disposal. For light atom transfer reactions, the following trends are found: $\Delta V \rightarrow \Delta V'$ and $\Delta T \rightarrow \Delta T' + \Delta R'$. Vibrational adiabaticity $\Delta V \rightarrow \Delta V'$ holds particularly well. Much less was known about the disposal of excess rotation.

For the $O(^3P) + HCl(v=2, J) \rightarrow OH(v', N') + Cl(^2P)$ reaction we observe strong product vibrational inversion and a substantial amount of product rotation. The available energy of reaction is nearly equipartitioned into product vibration, rotation, and translation. We have focused on the effect of reagent rotation on the product energy disposal and found that the energy disposal is independent of the rotation of the reagent. The large product rotation is consistent with a bent minimum energy path, in agreement with recent *ab initio* calculations.

ACKNOWLEDGMENTS

We would like to acknowledge D. J. Rakestraw for the quality of the setup and data acquisition system, and B. Gi-

rard for his help in the last phase of the experiment. W.J.vdZ. thanks the Netherlands Foundation for Scientific Research (Nederlandse Organisatie voor Wetenschappelijk Onderzoek) for a fellowship. This work is supported by the National Science Foundation under Grant No. NSF CHE 90-07939.

- ¹N. Sathyamurthy, *Chem. Rev.* **83**, 601 (1983).
- ²C.-K. Man and R. C. Estler, *J. Chem. Phys.* **75**, 2779 (1981).
- ³R. Altkorn, F. E. Bartoszek, J. deHaven, G. Hancock, D. S. Perry, and R. N. Zare, *Chem. Phys. Lett.* **98**, 212 (1983).
- ⁴R. Zhang, D. J. Rakestraw, K. G. McKendrick, and R. N. Zare, *J. Chem. Phys.* **89**, 6283 (1988).
- ⁵K. G. Anlauf, P. J. Kuntz, D. H. Maylotte, P. D. Pacey, and J. C. Polanyi, *Chem. Soc. Faraday Discuss.* **44**, 183 (1967).
- ⁶A. M. G. Ding, L. J. Kirsch, D. S. Perry, J. C. Polanyi, and J. L. Schreiber, *Chem. Soc. Faraday Discuss.* **55**, 252 (1973).
- ⁷D. J. Douglas, J. C. Polanyi, and J. J. Sloan, *J. Chem. Phys.* **59**, 6679 (1973).
- ⁸C. A. Parr, J. C. Polanyi, and W. H. Wong, *J. Chem. Phys.* **58**, 5 (1973).
- ⁹L. T. Cowley, D. S. Horne, and J. C. Polanyi, *Chem. Phys. Lett.* **12**, 144 (1971).
- ¹⁰J. C. Polanyi, *Acc. Chem. Res.* **5**, 161 (1972).
- ¹¹J. C. Polanyi and J. L. Schreiber, *Physical Chemistry an Advanced Treatise*, edited by H. Eyring, D. Henderson, and W. Jost (Academic, New York, 1974), Vol. VI A, Chap. 6.
- ¹²A. Persky and M. Broida, *J. Chem. Phys.* **81**, 4352 (1984).
- ¹³H. Kornweitz and A. Persky, *Chem. Phys.* **132**, 153 (1989).
- ¹⁴A. Persky and H. Kornweitz, *Chem. Phys. Lett.* **159**, 134 (1989).
- ¹⁵A. Persky and M. Broida, *Chem. Phys.* **114**, 85 (1987).
- ¹⁶M. Broida, M. Tamir, and A. Persky, *Chem. Phys.* **110**, 83 (1986).
- ¹⁷A. Persky and H. Kornweitz, *Chem. Phys.* **130**, 129 (1989).
- ¹⁸P. A. Elofson and L. Holmlid, *Chem. Phys. Lett.* **166**, 112 (1990).
- ¹⁹K. Schulten and R. G. Gordon, *J. Chem. Phys.* **64**, 2918 (1976).
- ²⁰G. C. Schatz, B. Amaee, and J. N. L. Connor, *Chem. Phys. Lett.* **132**, 1 (1986).
- ²¹P. L. Gertitschke, J. Manz, J. Römel, and H. H. R. Schor, *J. Chem. Phys.* **83**, 208 (1985).
- ²²M. Baer, *J. Chem. Phys.* **62**, 305 (1975).
- ²³H. Koizumi and G. C. Schatz, in *Molecular Vibrations*, edited by J. M. Bowman and M. A. Ratner (in press).
- ²⁴H. Koizumi and G. C. Schatz, *Int. J. Quant. Chem. Symp.* **23**, 137 (1989).
- ²⁵V. K. Babamov and R. A. Marcus, *J. Chem. Phys.* **74**, 1790 (1981).
- ²⁶J. Manz and J. Römel, *Chem. Phys. Lett.* **81**, 179 (1981).
- ²⁷I. W. M. Smith, *Acc. Chem. Res.* **23**, 101 (1990).
- ²⁸M. Kneba and J. Wolfrum, *Ann. Rev. Phys. Chem.* **31**, 47 (1980).
- ²⁹R. D. H. Brown and I. W. M. Smith, *Int. J. Chem. Kinet.* **7**, 301 (1975).
- ³⁰D. Arnoldi and J. Wolfrum, *Chem. Phys. Lett.* **24**, 234 (1974).
- ³¹R. D. H. Brown, G. P. Glass, and I. W. M. Smith, *Chem. Phys. Lett.* **32**, 517 (1975).
- ³²R. G. Macdonald and C. B. Moore, *J. Chem. Phys.* **68**, 513 (1978).
- ³³J. E. Butler, J. W. Hudgens, M. C. Lin, and G. K. Smith, *Chem. Phys. Lett.* **58**, 216 (1978).
- ³⁴R. D. H. Brown and I. W. M. Smith, *Int. J. Chem. Kinet.* **10**, 1 (1978).
- ³⁵D. J. Rakestraw, K. G. McKendrick, and R. N. Zare, *J. Chem. Phys.* **87**, 7341 (1987).
- ³⁶I. L. Childsey and D. R. Crosley, *J. Quant. Spectrosc. Radiat. Transfer* **23**, 187 (1980).
- ³⁷W. L. Dimpfl and J. L. Kinsey, *J. Quant. Spectrosc. Radiat. Transfer* **21**, 233 (1979).
- ³⁸R. A. Copeland, J. B. Jeffries, and D. R. Crosley, *Chem. Phys. Lett.* **138**, 425 (1987).
- ³⁹M. Troiler and J. R. Wiesenfeld (unpublished data for off-diagonal rotational line strengths).
- ⁴⁰C. H. Greene and R. N. Zare, *J. Chem. Phys.* **78**, 6741 (1983).
- ⁴¹J. Miyawaki, T. Tsuchizawa, K. Yamanouchi, and S. Tsuchiya, *Chem. Phys. Lett.* **165**, 168 (1990).
- ⁴²W. J. van der Zande, R. Zhang, H.-G. Rubahn, M. Bronikowski, and R. N. Zare (unpublished work).
- ⁴³C. E. Moore, *Atomic Energy Levels*, NSRDS-NBS, No. 35, 1971.

- ⁴⁴H. Zacharias, M. Geilhaupt, K. Meier, and K. H. Welge, *J. Chem. Phys.* **74**, 218 (1981).
- ⁴⁵H. Zacharias, K. Meier, and K. H. Welge, in *Energy Storage and Redistribution in Molecules*, edited by J. Hinze (Plenum, New York, 1983), p. 107.
- ⁴⁶W. J. van der Zande, R. Zhang, and R. N. Zare, in *Spectral Line Shapes* (American Institute of Physics, New York, in press), Vol. 6.
- ⁴⁷K. G. McKendrick, D. J. Rakestraw, R. Zhang, and R. N. Zare, *J. Phys. Chem.* **92**, 5530 (1988).
- ⁴⁸K. G. McKendrick, D. J. Rakestraw, and R. N. Zare, *Chem. Soc. Faraday Discuss.* **84**, 39 (1987).
- ⁴⁹H. Kornweitz, A. Persky, I. Schechter, and R. D. Levine, *Chem. Phys. Lett.* **169**, 489 (1990).
- ⁵⁰A. Jacobs, K. Kleinermanns, H. Kuge, and J. Wolfrum, *J. Chem. Phys.* **79**, 3162 (1983).
- ⁵¹M. J. Bronikowski, R. Zhang, D. J. Rakestraw, and R. N. Zare, *Chem. Phys. Lett.* **156**, 7 (1989).
- ⁵²G. C. Schatz (personal communication).
- ⁵³C. R. Park and J. R. Wiesenfeld, *Chem. Phys. Lett.* **163**, 230 (1989).
- ⁵⁴K. Kleinermanns, E. Linnebach, and M. Pohl, *J. Chem. Phys.* **91**, 2181 (1989).
- ⁵⁵In mass-weighted coordinates, the skew angle χ for O + HCl is 16.9° and for O + HB is 15.4°. See, I. W. M. Smith, *Kinetics and Dynamics of Elementary Gas Reactions* (Butterworth, London, 1980).
- ⁵⁶R. D. Levine and R. B. Bernstein, *Molecular Reaction Dynamics and Chemical Reactivity* (Oxford, New York, 1987).
- ⁵⁷K. Kleinermanns and A. C. Luntz, *J. Chem. Phys.* **77**, 3533, 3537, 3774 (1982).
- ⁵⁸I. Schechter and R. D. Levine, *J. Phys. Chem.* **93**, 7973 (1989).
- ⁵⁹M. S. Gordon, K. K. Baldrige, D. E. Bernholdt, and R. J. Bartlett, *Chem. Phys. Lett.* **158**, 189 (1989).